GRB Afterglows as a New ISM and IGM Probe

Hsiao-Wen Chen*, Jason X. Prochaska† and Josh S. Bloom**

*Department of Astronomy & Astrophysics, University of Chicago, Chicago, IL 60637, U.S.A.
†UCO/Lick Observatory, University of California at Santa Cruz, Santa Cruz, CA 95064, U.S.A.
**Department of Astronomy, University of California at Berkeley, Berkeley, CA 94720, U.S.A.

Abstract.
    We summarize results from a study of the metallicity, relative abundances, gas density, and kinematics of dense media in the host environment of two *Swift* bursts, GRB 050730 at $z = 3.968$ and GRB 051111 at $z = 1.549$. Both GRB hosts exhibit strong absorption features from excited Si^+ and Fe^+ ions, indicating an extreme ISM environment that is similar to what is found around massive stars like luminous blue variables (LBV) and Wolf-Rayet stars. The extreme ISM properties have never been observed in intervening quasar absorption line systems beyond the local universe.

1. UNVEILING EXTREME STAR-FORMING REGIONS

Mounting evidence has demonstrated that long-duration gamma-ray bursts (GRBs) arise in active star-forming regions [e.g. 1, 2], supporting a physical connection between the bursts and the catastrophic death of massive stars [3, 4]. Studies of the circumburst environment together with the progenitor stars therefore bear directly on our understanding of star formation and metal production in the early universe.

The extreme brightness of GRB optical afterglows, albeit brief, offers a unique means to unveil the physical conditions of the ambient medium around the burst progenitors. For example, low-resolution afterglow spectra have yielded a few diagnostic measurements such as the H I column density, the gas metallicity, and the dust-to-gas ratio of the GRB hosts [e.g. 8, 9]. High-resolution spectroscopy of the optical afterglows has further uncovered detailed kinematic signatures, population ratios of excited ions, and chemical compositions of the interstellar medium (ISM) and the circumstellar medium (CSM) of the progenitor star of the GRB [e.g. 5, 6, 7].

The majority of GRB host galaxies are known to have large neutral gas content with neutral hydrogen column density much beyond $\log N(\mathrm{H\,I}) = 20.3$ [e.g. 9], the standard threshold for selecting damped Lyα absorbers (DLAs). DLAs selected along random lines of sight toward background quasars dominate the mass density of neutral gas in the universe and represent a uniform sample of distant galaxies with known $N(\mathrm{H\,I})$. GRB host DLAs ($z_{\mathrm{DLA}} = z_{\mathrm{GRB}}$), which are presumably selected by vigorous star formation and therefore probe deep into the center regions of distant galaxies, presents a nice complement to classical DLA system ($z_{\mathrm{DLA}} < z_{\mathrm{GRB}}$), which arises preferencially at large galactocentric radii due to a larger cross-section of the outskirts than the inner regions. In this article, we summarize our analysis of the circumstellar medium observed in two GRB host galaxies, and compare with what is known for classical DLAs.
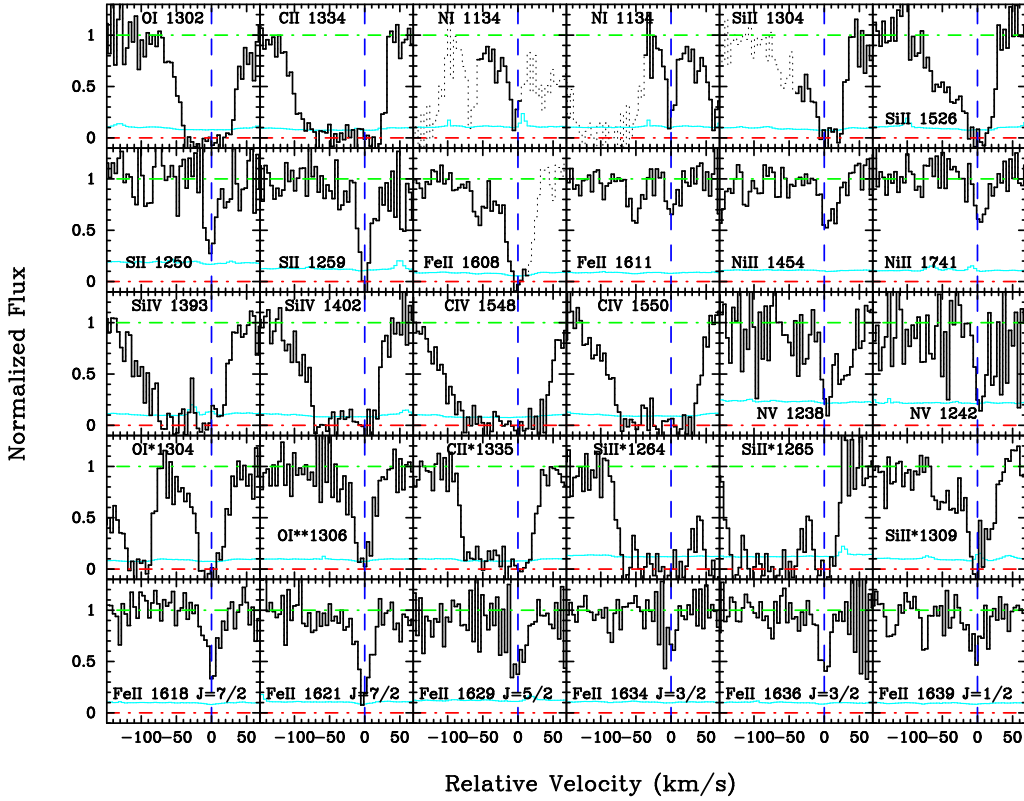
FIGURE 1. Absorption profiles of various ionic transitions found at the host redshift of GRB 050730. Resonance transitions are presented in the top three rows, while absorption features from excited O^0, C^+, Si^+, and Fe^+ are presented in the bottom two rows. Dotted curves indicate contaminating features that are not related to the marked transitions. The zero relative velocity corresponds to redshift $z = 3.96855$.

2. ABSORPTION-LINE PROPERTIES OF GRB HOSTS

High-resolution echelle spectra of GRB 050730 were obtained using the MIKE echelle spectrograph on the Magellan Clay telescope. The spectra cover a wavelength range from $\lambda = 3300$ Å to 9000 Å with a spectral resolution of FWHM ≈ 10 km s^{-1} at wavelength $\lambda = 4500$ Å and ≈ 12 km s^{-1} at $\lambda = 8000$ Å. We have identified a suite of metal-absorption lines at the redshift of the GRB $z = 3.96855$, including neutral species such as O I, low-ionization transitions such as C II, Si II, S II, Ni II, and Fe II, and high-ionization transitions such as C IV, Si IV, and N V. We have also identified strong fine-structure lines such as O I*, O I**, Si II*, C II*, and Fe II*.

Absorption profiles of these transitions are presented in Figure 1. The presence of strong fine-structure transitions indicate an extreme ISM environment with high gas density that is rarely observed in classical DLA systems. Furthermore, the profiles of well resolved lines (e.g. S II 1250) show that $> 90\%$ of the neutral gas is confined to a velocity width 20 km s^{-1}, which is considerably smaller than the median value of intervening DLA systems and implies a quiescent environment. The asymmetry of these line profiles is also suggestive of an organized velocity field, e.g. rotation or outflow.
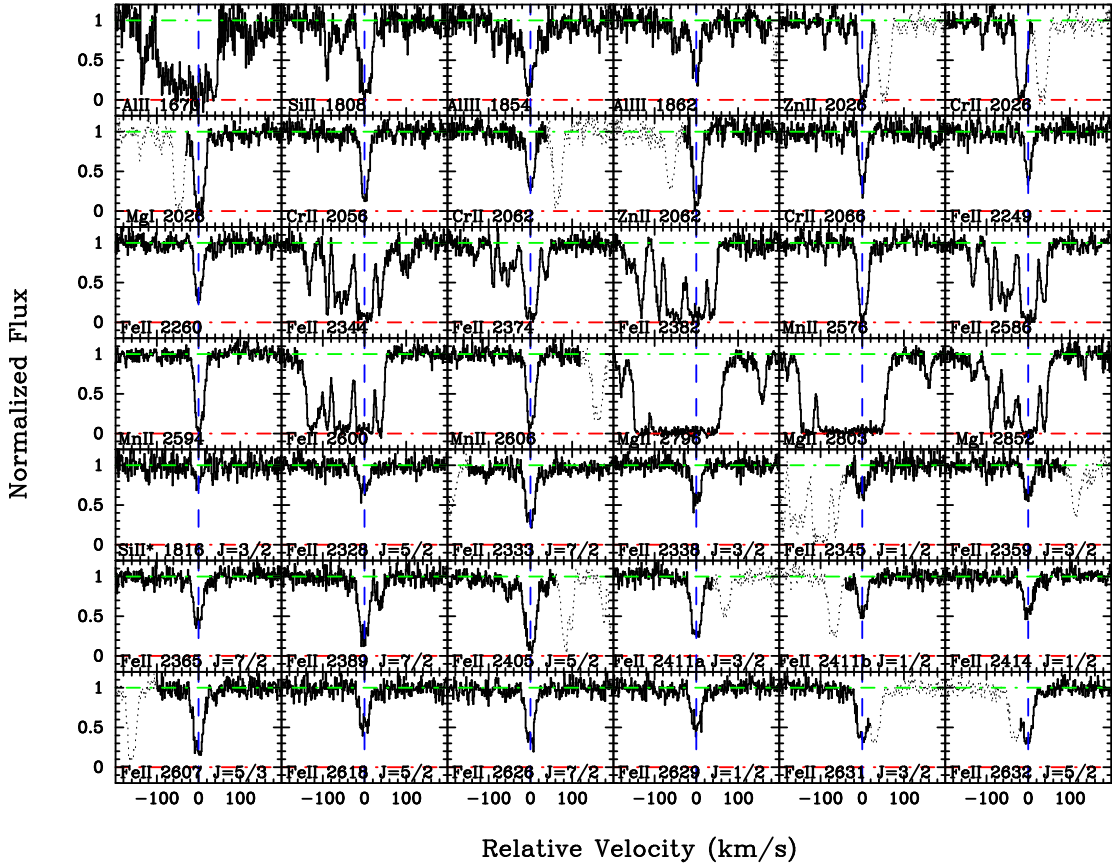
FIGURE 2. Absorption profiles of various ionic transitions found at the host redshift of GRB 051111. Resonance transitions are presented in the top four rows, while absorption features from excited Si^+, and Fe^+ are presented in the bottom three rows. The zero relative velocity corresponds to redshift $z = 1.54948$.

Additional properties measured for the host of GRB 050730 are summarized as follows. (1) We measure $\log N(\text{H I}) = 22.15 \pm 0.05$ and $[\text{S/H}] = -2.0 \pm 0.1$. Because S is non-refractory, its gas-phase abundance gives a direct measurement of the gas metallicity. (2) We find $[\text{S/Fe}] = +0.3$, consistent with the gas phase $[\alpha/\text{Fe}]$ measurements of low-metallicity DLA systems. Even if we adopt an intrinsic solar abundance pattern, the dust-to-gas ratio in the host ISM is very low [c.f. 8]. (3) We measure $[\text{N/S}] = -1.0 \pm 0.2$, again consistent with low-metallicity DLA systems. (4) We detect no molecular lines in the Lyα forest with a 3-σ upper limit to the molecular fraction $f_{\text{H}_2} \equiv 2N(\text{H}_2)/[2N(\text{H}_2) + N(\text{H I})] < 10^{-8}$. The lack of H_2 suggests a warm gas phase, consistent with the implication from the detections of excited Si^+ and Fe^+.

High-resolution echelle spectra of GRB 051111 were obtained using the High Resolution Echelle Spectrometer (HIRES) on the Keck I telescope. The spectra cover a wavelength range from $\lambda = 4165 - 8720$Å with a spectral FWHM resolution of ≈ 5km s^{-1}. We have identified a suite of metal absorption lines at the redshift of the GRB $z = 1.54948$, including resonance transitions such as Si I, Mg I, Zn II, Cr II, Mg II, Fe II, Mn II, and Al III, as well as fine-structure transitions due to excited Si^+ and Fe^+.

Absorption profiles of these transitions are presented in Figure 2. We find that while

saturated lines such as Fe II, Mg I and Mg II exhibit multiple components over a velocity range from -140 km s^{-1} to 40 km s^{-1}, well resolved lines such as Cr II and weak Fe II show that $> 90\%$ of the neutral gas is confined to a velocity width 30 km s^{-1}. In addition, the Si II 1808 and Zn II 2026,2062 transitions are saturated, indicating $\log N(\text{Zn}) > 13.5$ and $\log N(\text{Si}) > 15.9$. These measurements represent by far the largest Zn and Si column densities observed in QSO absorption line systems. The presence of Fe$^+$ in all four excited ^6D_J states with $J = 7/2, 5/2, 3/2$, and $1/2$ suggests a large gas density in the absorbing medium. The weak Mg I 2026 transition appears to be saturated, indicating a warm gas of temperature $T > 1000$ K.

The hydrogen Lyα transition of GRB 051111 is not observed in the ground-based data. Adopt the observed lower limit to the Zn abundance $\log N(\text{Zn}) > 13.5$, we estimate $\log N(\text{H I}) > 20.8$ for gas of solar metallicity. Lower metallicity would lead to higher $N(\text{H I})$ for the neutral gas content in the host ISM. In addition, the observed Zn to Fe ratio is $[\text{Zn/Fe}] > 1.2$. This large ratio suggests significant differential depletion in the host of GRB 051111, contrary to what is observed for the host of GRB 050730.

3. CIRCUMBURST ENVIRONMENT OF GRB PROGENITORS

An emerging feature of GRB progenitor environments is the presence of strong fine-structure transitions from excited states of C$^+$, Si$^+$, O^0, and Fe$^+$. In contrast to resonance transitions of the dominant ions in neutral gas, these absorption lines can reveal the temperature and density of the gas, as well as the ambient radiation field. In particular, detections of Fe II fine structure transitions have only been reported in rare places such as broad absorption-line (BAL) quasars, η Carinae and the circumstellar disk of β Pictoris. Identifications of strong Fe II fine-structure transitions therefore suggest extreme gas density and temperature in the GRB progenitor environment.

We examine the excitation mechanism and gas density of the absorbing medium through comparisons of the observed relative abundances between different excited states of the Fe$^+$ ion. The population ratios between different states are determined based on the balance between excitation and de-excitation rates. When the density is sufficiently large that the collisional de-excitation rates exceed the spontaneous decay rate, the excited states are populated according to a Boltzmann distribution,

$$\frac{n_i}{n_j} = \frac{g_i}{g_j} \exp[-(E_{ij}/k)/T_{Ex}], \tag{1}$$

where g_i is the degeneracy of state i, $E_{ij} \equiv E_i - E_j$ is the difference in energy between the two states, and T_{Ex} is the excitation temperature.

Figure 3 shows the observed column density N_i scaled by the corresponding degeneracy g_i for each of the Fe$^+$ excited states as a function of the energy E_{ij} above the ground state $J = 9/2$. The error bars reflect 1-σ uncertainty in N_i. The solid (blue) curve indicates the best-fit Boltzmann function with a best-fit excitation temperature $T_{\text{Ex}} = 6100$ K for GRB 050730 and $T_{\text{Ex}} = 2600$ K for GRB 051111. The inset shows the minimum χ^2 values as a function of T_{Ex}. The reduced χ^2 is nearly unity, $\chi^2_\nu = 1.02$, supporting our assumption that the Boltzmann function is a representative model.
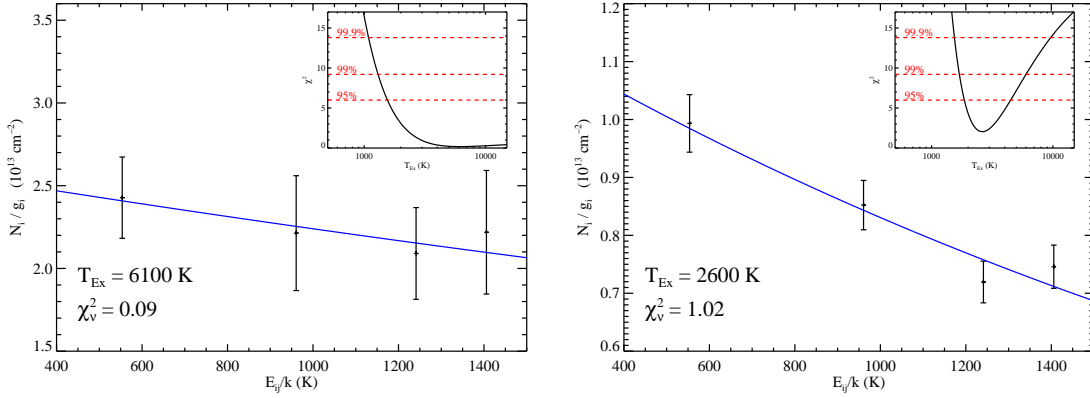
FIGURE 3. Relative abundance ratios between different excited Fe II states, N_i/g_i where g_i represents the degeneracy of the corresponding level, as a function of their energy E_{ij} above the ground state. We present measurements for the host of GRB 050730 in the left panel and GRB 051111 in the right panel. The solid curve in each panel represents the best-fit function $A\exp[-(E_{ij}/k)/T_{Ex}]$ for a minimum χ^2 value. We find a best-fit excitation temperature $T_{Ex} = 6100$ K for GRB 050730 and $T_{Ex} = 2600$ K for GRB 051111. The insets show the reduced χ^2 values for a range of T_{Ex} values.

Adopting the best-fit temperature for the absorbing medium, we can further constrain the electron density based on the observed column density ratios. We calculate the expected population ratio between excited fine-structure states i and ground state $J = 9/2$ for gas of $T = 6100$ K and $T = 2600$ K, using the PopRatio software package [10]. We find that $n_e > 1000\,\mathrm{cm}^{-3}$ for both systems. To estimate the total gas density n_H based on the estimated n_e requires knowledge of the ionization state of the absorbing gas traced by the excited Fe^+. The large $N(\mathrm{H\,I})$ estimated for both systems implies an optical depth to ionizing radiation ($h\nu > 1\mathrm{Ryd}$) $\tau > 1000$. While an O or B star (or the GRB itself) could significantly ionize a skin-layer on the outside of the cloud, the majority of the gas would remain neutral. Therefore, the hydrogen gas must be predominantly neutral and we can safely assume an ionization fraction $x < 10^{-2}$. We therefore infer $n_H > 10^5$ cm^{-3} for the absorbing medium, which further leads to an upper limit to the size of the excited medium $\ell = N(\mathrm{H\,I})/n_H < 10^{17}$ cm, i.e., less than 1/3 pc.

This small dimension implies that it must arise near the GRB event (at $r \sim \ell$) or have a nearly unity covering fraction at large radii (e.g. a thin shell). Additional constraints can be derived based on absorption features due to neutral species and the afterglow light curves. A detailed discussion is presented in Prochaska, Chen, & Bloom (2006).

4. CLASSICAL DLAS VERSUS GRB HOSTS

A striking feature is that both GRB hosts exhibit Fe^+ and Si^+ fine-structure transitions which have never been observed in intervening quasar absorption line systems [e.g. 11]. Figure 4 presents a sharp contrast in the line strengths of different excited ions observed in a classical DLA with $\log N(\mathrm{H\,I}) = 21.3$ at $z = 2.6264$ and in the host of GRB 050730. Our study shows that aside from having a much higher neutral gas density and temper-
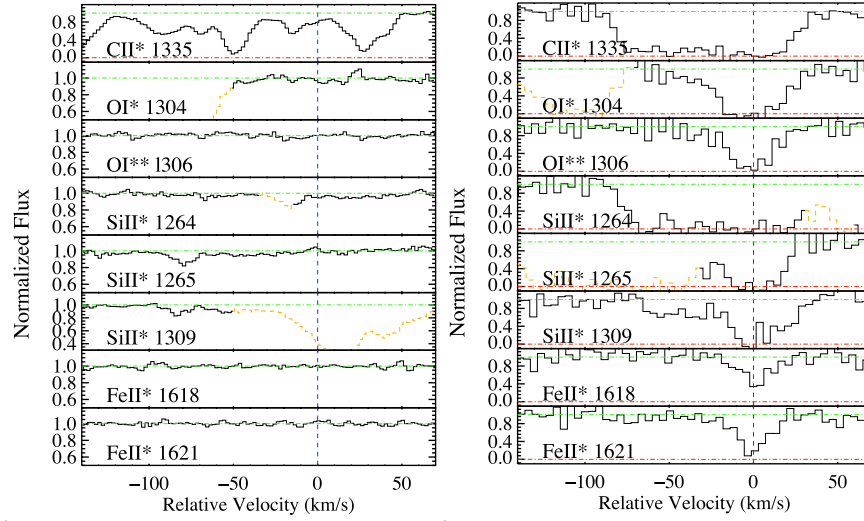
FIGURE 4. Comparisons of line strengths due to different excited ions observed in a classical DLA with log $N(\text{H I}) = 21.3$ at $z = 2.6264$ (left panel) and in the host of GRB 050730 (right panel).

ature as derived from the observed population ratios between different excited ions, the GRB hosts have very similar characteristics to known DLA systems at $z > 2$, such as low dust content, low metallicity, and α-element enhanced chemical composition.

As bright lighthouses for high-resolution optical spectroscopy, GRBs are now fulfilling their promise as detailed complementary probes of the distant universe. It is only a matter of time when high- resolution spectroscopy at **infrared** wavelengths will afford an picture of star formation and chemical enrichment in the epoch of reionization.

ACKNOWLEDGMENTS

REFERENCES

1. Bloom, J. S. et al. 2002, ApJ, 572, L45
2. Stanek, K. Z. et al. 2003, ApJ, 591, L17
3. Woosley, S. E. 1993, ApJ, 405, 273
4. Paczyński, B. 1998, ApJ, 494, 45
5. Fiore, F. et al. 2005, ApJ, 624, 853
6. Chen, H.-W., Prochaska, J. X., Bloom, J. S., & Thompson, I. B. 2005, ApJ, 634, L25
7. Prochaska, J. X., Chen, H.-W., & Bloom, J. S. 2006, submitted to ApJ (astro-ph/0601057)
8. Savaglio, S., Fall, S. M., & Fiore, F. 2003, ApJ, 585, 638
9. Vreeswijk, P. M. 2004, A&A, 419, 927
10. Silva, A. I. & Viega, S. M. 2002, MNRAS, 329, 135

11. Howk, J. C., Wolfe, A. M., & Prochaska, J. X. 2005, ApJ, 622, L81